scientific reports

Check for updates

OPEN

Tilia species (linden) exert anti-cancer effects on MIA PaCa-2 cells through the modulation of oxidative stress and inflammation

Gamze Yüksel[1], Yağmur Özhan[1], Dilara Güreşçi[1], Etil Güzelmeriç[2], Nisa Beril Şen[2], İpek Bedir[3], Onur Senol[4], Gizem Emre[5], Dilek Telci[3], Vilma Petrikaitė[6,7] & Hande Sipahi[1]✉

This study investigated the anti-cancer effects of the chemically characterized *Tilia* species (linden) on MIA PaCa-2 cells by analyzing various cancer-triggering mechanisms, including oxidative stress and inflammation status. Extracts from the flowers, bracts, and inflorescences of *T. cordata*, *T. platyphyllos*, *T. rubra*, and *T. tomentosa* were evaluated for antioxidant activity; subsequently, their ability to mitigate inflammation was assessed through *in vitro* nitrite assays in LPS-induced RAW264.7 cells. The anticancer potentials of the extracts against MIA PaCa-2 pancreatic cancer cells were investigated in 2D (cytotoxic effect) and 3D (effect on spheroid growth) models *in vitro*. All investigated *Tilia* species displayed remarkable antioxidant activity and significantly inhibited LPS-induced nitrite, IL-6, and PGE_2 production. Extract from *T. rubra* bracts showed the highest cytotoxic activity against MIA PaCa-2 cells with an IC_{50} value of 0.16 mg/mL, as well as the most significant delay on spheroid growth, which was further confirmed through the arrest in cell cycle. In the Annexin V cell death assays of *T. rubra*, cells treated with the flower extract exhibited the highest rate of necrotic population with 66.53%. Overall, our results highlight a potential use for *Tilia* extracts, particularly *T. rubra*, in pancreatic cancer treatment by modulating cell death.

Keywords *Tilia* species, Phenolic profile, Antioxidant activity, Anti-inflammatory activity, Anticancer activity, 3D spheroid model

Abbreviations

CUPRAC	Cupric reducing antioxidant capacity
DAD	Diode array detector
DMEM	Dulbecco's modified eagle's medium
DNA	Deoxyribonucleic acid
DOX	Doxorubicin
DPPH	2,2-diphenyl-1-picrylhydrazyl
ELISA	Enzyme-linked immunosorbent assay
FBS	Fetal bovine serum
FRAP	Ferric ion reducing antioxidant power
GAE	Gallic acid equivalent
HPLC	High-performance liquid chromatography
HPTLC	High-performance thin layer chromatography
IC50	The half maximal inhibitory concentration
IL-6	Interleukin-6
LPS	Lipopolysaccharide
2D	Two-dimensional

[1]Faculty of Pharmacy, Department of Toxicology, Yeditepe University, 34755 Istanbul, Türkiye. [2]Faculty of Pharmacy, Department of Pharmacognosy, Yeditepe University, 34755 Istanbul, Türkiye. [3]Department of Genetics and Bioengineering, Yeditepe University, 34755 Istanbul, Türkiye. [4]East Anatolian High Technology Research and Application Center (DAYTAM), Atatürk University, 25240 Erzurum, Türkiye. [5]Faculty of Pharmacy, Department of Pharmaceutical Botany, Marmara University, 34854 Istanbul, Türkiye. [6]Lithuanian University of Health Sciences, LT-44307 Kaunas, Lithuania. [7]Life Sciences Center, Institute of Biotechnology, Vilnius University, LT-10257 Vilnius, Lithuania. ✉email: hande.sipahi@yeditepe.edu.tr; handesipahi@hotmail.com

3D	Three-dimensional
MeOH	Methanol
MTT	3-(4,5-dimethylthiazol-2-yl)-2,5-diphenyltetrazolium bromide
PBS	Phosphate buffer saline
PEG 400	Polyethylene glycol 400
PGE_2	Prostaglandin E2
PI	Propidium Iodide
QE	Quercetin equivalent
RNase A	Pancreatic ribonuclease
ROS	Reactive oxygen species
TE	Trolox equivalent
TFC	Total flavonoid content
TLC	Thin-layer chromatography
TPC	Total phenolic content
TPTZ	2,4,6-tris(2-pyridyl)-s-triazine
UV-Vis	Ultraviolet-visible

Introduction

Cancer is a multi-stage disease that involves uncontrolled cell proliferation and mutations. Based on the molecular, cellular, and pathologic aspects of the transforming of a normal cell into a neoplastic lesion, the multistage processes leading to cancer development involve initiation, promotion, and progression stages[1]. Oxidative stress, which is defined as an imbalance between the production of free radicals and reactive oxygen species (ROS), is one of the major causes of these three stages. ROS may damage DNA at the beginning stage by introducing structural changes and gene mutations. During the promotion phase, ROS may play a role in aberrant gene expression, disruption of intercellular communication, and alteration of second-messenger systems. These outcomes may lead to either an increase in cell division or a reduction in the apoptosis of the initial cell population[2,3]. Additionally, ROS represent a link between chronic inflammation and cancer. Inflammatory cells that release ROS may also cause DNA damage. Indeed, numerous stages of the carcinogenesis process, such as cellular transformation, promotion, survival, proliferation, invasion, angiogenesis, and metastasis, have been connected to chronic inflammation and oxidative stress[1,2]. The use of medicinal plants has become a limelight for their potential to mitigate oxidative stress-related diseases, alleviate inflammatory conditions, and even combat cancer, stating their promise as a natural remedy with multifaceted health benefits.

Tilia species known as linden or lime trees, are found in Türkiye as *Tilia cordata* Mill., *Tilia tomentosa* Moench, *Tilia rubra* DC., and *Tilia platyphyllos* Scop. The light to dark green-colored leaves of *Tilia* species are alternate and have cordate and asymmetric lamina with dentate- or serrate-shaped margins. The yellowish-colored flowers in inflorescence bloom between June and July. The peduncle (the main stalk of the inflorescence) is adherent to long and oblong-lanceolate shaped bracts from the bottom to the middle, and they grow together. The number of flowers in the inflorescence varies from two to ten, depending on the species[4]. Traditionally, brewed flowers or inflorescences comprising flowers and bracts of *Tilia* spp. have been used to treat common cold and cough[5]. Additionally, scientific studies have shown their sedative, antioxidant, neuroprotective, antiproliferative, antimicrobial, antitussive, and immunomodulating activities. These effects are attributed to its flavonoids (derivatives of kaempferol and quercetin), phenolic acids, volatile oil, and polysaccharide components[6–9]. Astragalin and tiliroside, which were initially isolated from the leaves of *T. tomentosa*, are responsible for various pharmacological activities of *Tilia* species, including antioxidant, anti-inflammatory, hepatoprotective, neuroprotective, antithrombotic, antidiabetic, antiobesity, antiviral, antiosteoporotic, and antiproliferative activities[6,7]. Additionally, quercetin derivatives such as hyperoside, quercitrin, and isoquercitrin have a broad spectrum of biological activities, including anticancer, anti-inflammatory, antibacterial, antiviral, antidepressant, and organ protective effects[10,11]. Apart from flavonoids, alkaloids such as tiliine A, tiliamine B, and tilacetine A found in the mixture of *T. platyphyllos* and *T. cordata* may act as acetylcholinesterase inhibitors[12].

Previously, the anti-cancer properties of *T. platyphyllos* were evaluated against different cell lines such as HeLa (cervix cancer), HepG2 (hepatocellular carcinoma), NCI-H460 (lung carcinoma), and MCF-7 (breast adenocarcinoma)[13]. Other studies examined the antiproliferative effect of *T. cordata* extracts on LS180 (human colon adenocarcinoma) and BW 5147 (lymphoma tumor) cells dose dependently[14,15]. *T. tomentosa* extract has been shown to be effective in lung adenocarcinoma A549 cell line[16]. In the literature search, no studies were found on the anticancer activity of *T. rubra*. Besides, among these studies, there is no comparative evaluation of different *Tilia* species, including *T. cordata*, *T. tomentosa*, *T. rubra*, and *T. platyphyllos*, regarding their antioxidant activity, protective role against inflammation, and anticancer potentials. Furthermore, the effect of *Tilia* species on pancreatic cancer remains inconclusive. Pancreatic cancer is the seventh leading cause of cancer-related deaths in the world and is expected to be third by 2025 with poor diagnosis and occurs in both genders[17].

The primary aim of this study was to assess the anti-cancer properties of the hydroethanolic extracts of different *Tilia* species using the MIA PaCa-2 pancreatic cancer cell line by investigating the status of various cancer-triggering mechanisms, including oxidative stress and inflammation. To study the anti-cancer potential, cytotoxicity on the cell monolayer (2D model), effect on 3D spheroid growth, and apoptosis assays were also conducted. To further characterize and quantify the main phenolic components, high-performance thin-layer chromatography (HPTLC) and high-performance liquid chromatography (HPLC) were used to determine the components underlying the aforementioned biological activities.

Materıals and methods

Chemicals and solvents

The brands of chemicals and solvents used during the analyses, along with their abbreviations, are listed in the 'Materials and Methods' section of Supplementary Information.

Plant materials

Tilia species were collected during the flowering stages, from May to June: *T. cordata* was collected from Şile-İstanbul, Türkiye (41.1749° N, 29.6096° E); *T. platyphyllos* from Bayramiç-Çanakkale, Türkiye (39.8095° N, 26.6120° E); *T. tomentosa* from Serhat Köyü-Bayramiç-Çanakkale, Türkiye (39.7397° N, 26.7064° E); and *T. rubra* from Turgutlu-Manisa, Türkiye (38.5002° N, 27.7084° E). The specimens were authenticated by Assoc. Prof. Gizem Emre using the Flora of Turkey and the East Aegean Islands (Davis, 1965–1985). The voucher specimens for *T. cordata* Mill. (MARE 22872), *T. platyphyllos* Scop. (MARE 22871), *T. tomentosa* Moench (MARE 22727), and *T. rubra* DC. subsp. *caucasica* (Rupr.) V. Engler (MARE 2272a) are stored at the Herbarium of Marmara University Faculty of Pharmacy (MARE), İstanbul, Türkiye. All plant parts were dried at room temperature and stored in appropriate conditions until analysis.

Preparation of sample and standard solutions

Five grams of powdered flowers, bracts, and inflorescence containing bracts and flowers (1:1 *w*/*w*) were extracted with an 80% ethanol$_{(aq)}$ solution, and each sample was ultrasonicated for 30 min. Then the samples were filtered through a filter paper and a syringe filter (pore size 0.45 µm). Ethanol was completely evaporated in a rotary evaporator (BÜCHI Labortechnik, Flawil, Switzerland) under reduced pressure at 40°C. Finally, the remaining part was lyophilized. The sample stock solutions were prepared using 80% ethanol at a concentration of 20 mg/mL. The solutions were further diluted using the same solvent for the antioxidant assays and HPTLC and HPLC analyses.

The stock solutions of protocatechuic acid, hyperoside, isoquercitrin, astragalin, quercitrin, and tiliroside were prepared in methanol at a concentration of 300 µg/mL. Equal volumes of each stock solution were mixed to prepare a standard mixture solution (50 µg/mL) used for the HPTLC analysis.

Prepared sample test solutions and standard solutions were stored at 4 °C during the analyses.

Chemical characterization of Tilia species

– **HPTLC analysis**

Samples (20 mg/mL) and standard mixture solution (50 µg/mL) were applied on an HPTLC silica gel 60 F_{254} glass plate (20 × 10 cm, Merck, Darmstadt, Germany) in 4 µL and 2 µL volumes, respectively, using a semi-automatic sample spotter Linomat 5 (Camag, Muttenz, Switzerland). The plate was developed using a developing solvent system containing ethyl acetate-formic acid-water (30:3:3, *v*/*v*/*v*) up to a migration distance of 7 cm in 20 min in a saturated twin trough chamber (Camag) to separate the investigated compounds in the sample test solution. After development, the plate was dried by exposure to cold air. Then, the plate was heated at 105 °C for 3 s on a TLC plate heater (Camag). Next, the plate was dipped into a solution containing 2-aminoethyl-diphenylborinate in ethyl acetate (Natural Product, NP) and polyethylene glycol (PEG) 400 in dichloromethane, respectively. Finally, the plate was documented at 366 nm using the Camag TLC visualizer. All steps were operated by the winCATS program (version 1.4.8, Camag).

– **HPLC analysis**

The chromatographic separations were performed using the Agilent 1260 Infinity HPLC system with a diode array detector (DAD), which has a vacuum degassing system, an automatic sampler, a thermostatted column compartment, and a quaternary pump. The Agilent Chem Station software was used for analysis. An Agilent Zorbax Plus C 18 column (4.6 mm × 250 mm) with a 5 µm particle size was employed to provide optimal conditions to separate the investigated compounds. The best separation was obtained with a 1 mL/min flowing rate at 25 °C. Ultra-purified water with 0.1% *o*-phosphoric acid and acetonitrile were used as mobile phases A and B, respectively. The gradient profile was as follows: 85–15% A-B (0–3 min), 82–18% A-B (3–11 min), 80–20% B (11–16 min), 70–30% A-B (16–22 min), 50–50% A-B (22–25 min), 20–80% A-B (25–26 min), and 85–15% A-B (26–30 min). A volume of 10 µL was injected for standard solutions and samples, and each injection was performed in triplicate. Different wavelengths were used to monitor the analytes. These values were selected according to their UV_{max} values. Protocatechuic acid, hyperoside, isoquercitrin, and quercitrin were monitored at 260 nm, whereas astragalin and tiliroside were monitored at 265 and 320 nm, respectively.

The linearity data of the calibration curve, along with the values for the LOQ and LOD, are provided in Supplementary Table S1. Repeatability and precision data for standards are presented in Supplementary Table S2, and recovery results are given in Supplementary Table S3.

– **Total phenolic content estimation by the Folin–Ciocalteu method**

The total phenolic content (TPC) of the samples was evaluated using the Folin–Ciocalteu reagent method described by Singleton et al. (1999), with a slight modification[18]. Firstly, 50 µL of different concentrations of gallic acid standard solutions (3.125–100 µg/mL), sample test solutions that belong to *Tilia* samples, and blank were placed into each well separately in a 96-well plate and mixed with 50 µL of 10% Folin–Ciocalteu reagent. Then, 100 µL of 7.5% (*w*/*v*) Na_2CO_3 was added to these mixtures. The prepared mixtures were kept in the dark for 30 min at room temperature. The absorbance was measured using a UV/Vis spectrophotometer (Multiscan

Go, Thermo Scientific) at 760 nm. All analyses were performed in triplicate, and the TPCs of the samples were calculated according to the obtained calibration curve by gallic acid standards and expressed as mg of gallic acid equivalents (GAE) per g of hydroethanolic *Tilia* extract (mg GAE/g hydroethanolic *Tilia* extract).

– **Evaluation of total flavonoid content**

The total flavonoid content (TFC) in *Tilia* samples was determined by a slightly modified method stated by Farasat et al. (1999)[19]. 30 µL of each sample test solution, quercetin standard solutions, and blank (MeOH) were first placed in separate wells of a 96-well plate, and 30 µL of 10% aluminum chloride and 30 µL of 1 M sodium acetate were added, respectively. Finally, the volume was adjusted to 240 µL with distilled water. After 30 min of incubation at room temperature, the absorbance was measured at 415 nm using a UV/Vis spectrophotometer. All analyses were performed in triplicate, and the total flavonoid content of the *Tilia* samples was expressed as mg quercetin equivalents (QE) per g of hydroethanolic *Tilia* extract (mg QE/g hydroethanolic *Tilia* extract).

Biological activities

– **Free radical-scavenging activity with 2,2-diphenyl-1-picrylhydrazyl (DPPH) assay**

DPPH radical scavenging activity was measured using a slightly modified version of the method stated by Blois et al. (1957)[20]. To perform the analysis, 20 µL of *Tilia* sample test solutions, trolox standard solutions in a range of 3.125–200 µg/mL, and blank (MeOH) were added in a 96-well plate separately, and each was mixed with 280 µL of DPPH solution (0.1 mM). After 30 min of incubation in a dark environment at room temperature, absorbance was measured at 520 nm using a UV/Vis spectrophotometer. The results were presented in mg Trolox equivalent (TE)/g of hydroethanolic *Tilia* extract (mg TE/g hydroethanolic *Tilia* extract).

– **Metal-reducing activity by cupric-reducing antioxidant capacity (CUPRAC) assay**

To perform the CUPRAC assay, 85 µL of 10 mM copper (II) sulfate pentahydrate, 85 µL of 7.5 mM neocuproine, 85 µL of ammonium acetate buffer solution (pH = 7), and 51 mL of distilled water were added to the 96-well microplate, respectively. Then, either 43 µL of each sample test solution or standard solution (3.125–200 µg/mL) or water as a blank was placed in each well. After incubation of the plate at room temperature for 30 min at 50 °C, the absorbance was read at 450 nm[21]. The results were given in mg Trolox equivalent (TE)/g of hydroethanolic *Tilia* extract (mg TE/g hydroethanolic *Tilia* extract).

– **Metal-reducing activity by ferric-reducing antioxidant power (FRAP) assay**

For the analysis, 20 µL of sample test solution, standard solutions in the range of 3.125–100 µg/mL, and blank (distilled water) were added to a 96-well plate separately, and each well was mixed with 280 µL of FRAP reagent [2,4,6-tri(2-pyridyl)-s-triazine (TPTZ; 0.01 M) solution, acetate buffer (pH = 3.6) solution, and 0.02 M iron (III) chloride hexahydrate solution were mixed at a 10:1:1 ratio]. After 6 min, the absorbances were determined at 595 nm[22]. The results were expressed in mg Trolox equivalent (TE)/g of hydroethanolic *Tilia* extract (mg TE/g hydroethanolic *Tilia* extract).

Cell culture studies

Evaluation of the protective effect against inflammatory response

– **Cell viability**

RAW264.7 mouse macrophage cells were obtained from the American Type Culture Collection (ATCC, Rockville, MD) and cultured in Dulbecco's Modified Eagle's Medium (DMEM) (Gibco, NY, USA) enriched with 1% penicillin (10.000 units/mL) and streptomycin (10.000 µg/mL) and 10% fetal bovine serum (FBS) (Gibco™, USA) at 37 °C in a humidified atmosphere of 5% CO_2.

The MTT colorimetric assay was used for the cytotoxicity analysis according to the method described by Sipahi et al. (2022)[23]. The plated cells were treated with four different concentrations of *Tilia* species extracts (0.125–1 mg/mL). Indomethacin (IND) and L-NAME (Nv-Nitro-L-arginine methyl ester hydrochloride) (100 µM) (Sigma Aldrich, St. Louis, MI, USA) was used as a positive control for evaluation of the protective effect against inflammatory response and analgesic activity. The plates with treated cells were then incubated for 24 h. After removal of the medium, MTT reagent (0.5 mg/mL) was applied, and the cells were incubated for another 2 h. The medium was then removed, and formazan crystals were dissolved in 100 µL of isopropanol. The absorbance was measured with a microplate reader (Thermo Multiscan Spectrum, Vantaa, Finland) at 570 nm wavelength. The test procedure was performed in triplicate. The cell viability in percentages was determined with the following equation:

Viability of cell (%) = $100 \times OD_{570test}/OD_{570control}$.

$OD_{570test}$: Mean value of measured optical density of the tested substance.

$OD_{570control}$: Mean value of measured optical density in the negative control group.

Further experiments were conducted at safe doses of extracts where the determined percent cell viability was 70% or higher compared with the control.

– **Determination of nitrite levels**

RAW264.7 cells seeded in a 96-well plate at a density of 5×10^4 cells/well were incubated at 37 °C in 5% CO_2 for 24 h. Cells were then pretreated with different concentrations of *Tilia* extracts (0.125–1 mg/mL) for 2 h. After that, cells were stimulated with LPS (1 µg/mL) for 22 h. The supernatant was collected, and 50 µL of the supernatant was mixed with 50 µL of the Griess reagent. Then, the mixture was incubated for 10 min in the dark. The absorbance was determined at 540 nm spectrophotometrically with a microplate reader (Multiscan Ascent, Vantaa, Finland)[24].

– **IL-6 releasing ınhibition assay**

IL-6 levels were tested at the highest non-cytotoxic extract dose. The manufacturer's recommendations were followed while utilizing a commercially available quantitative enzyme-linked immunosorbent assay (ELISA) kit (Invitrogen, USA) to measure the quantity of IL-6 in cell culture supernatant. Given the high IL-6 value of the samples, dilution was performed five times[25]. The results were expressed as pg/mL.

– **Evaluation of analgesic activity with prostaglandin E2 (PGE_2) levels**

PGE_2 levels were tested at the highest non-cytotoxic extract dose. Using an ELISA kit from Abcam (USA), the release of PGE_2 from cell supernatants was measured in duplicates in accordance with the manufacturer's instructions. The results were expressed as pg/mL[26].

Anticancer activity

– **Two-dimensional (2D) cell cytotoxicity assay**

Human pancreatic cancer cell line MIA PaCa-2 (CRM-CRL-1420) and human dermal fibroblast cell line HDF (PCS-201-012) were obtained from the American Type Culture Collection (ATCC, USA). Cell lines were cultured in Dulbecco's Modified Eagle's Medium supplemented with 10% FBS, 1% penicillin (10.000 units/mL), and streptomycin (10.000 µg/mL) at 37 °C under a humidified atmosphere of 5% CO_2[27].

To determine 2D anticancer activity, MIA PaCa-2 and HDF cells (10^4 cells/well) were seeded in a 96-well cell culture plate and allowed to attach for 24 h. To determine non-cytotoxic concentrations, cells were treated with *Tilia* extracts at four different concentrations (0.125, 0.25, 0.5, and 1 mg/mL) and incubated for 24 h. The culture medium was then removed, the MTT assay reagent (0.5 mg/mL) was added to all wells, and the cells were incubated for 2 h at 37 °C. Next, the culture medium was removed, and, in order to dissolve formazan crystals, 100 µL of isopropanol was added into the wells. The absorbance was measured at 570 nm wavelength with an ELISA microplate reader (Thermo Multiskan Spectrum, Finland). Cell viability was calculated as percentages using the following equation:

$$\text{Viability\%} = (\text{Absorbance}_{\text{treatment group}})/(\text{Absorbance}_{\text{ontrol}}) \times 100\%.$$

The IC_{50} values of *Tilia* extracts were calculated via the ECIC function code inserted into Microsoft Excel.

– **Three-dimensional (3D) spheroid formation/growth assay**

For 3D spheroid formation, MIA PaCa-2 and HDF cells were used according to the magnetic 3D Bioprinting method[28]. Human fibroblasts were mixed equally with pancreatic cancer cells to better stimulate the tumor environment. After cells reached 70–80% confluency, cells were treated with biocompatible NanoShuttle™-PL (Bioprinting Kit, Greiner Bio-One, Germany) and incubated overnight. Then, the cells were resuspended and seeded into ultra-low attachment 96-well culture plates with a 100 µL (2.000 pancreatic cancer cells and 2.000 human fibroblasts per well) volume[29]. Until spheroids were formed, the culture plate was placed on a magnetic drive and incubated in a humidified atmosphere containing 5% CO_2 at 37 °C for 48 h. Two days after the incubation period, the spheroids were photographed using light microscopy (Carl Zeiss Primo Vert, Germany). After that, spheroids were treated with flower, bract, and inflorescence of *T. cordata*, *T. tomentosa*, *T. rubra*, and *T. platyphyllos* extracts with the same concentration interval tested in RAW264.7 cells (0.125–1 mg/mL). For 10 days, treatment media were replaced with fresh media, and images of spheroids were captured every 3 days. The effect of *Tilia* extracts on spheroid growth was assessed by measuring the size change of spheroids using ImageJ software (Image J.2.0 software, USA). Doxorubicin (DOX) was used as a comparator (10 µM). All the measurements were performed in triplicate.

Cell cycle arrest

MIA PaCa-2 human pancreatic carcinoma cells were seeded in 6-well plates at a density of 3×10^5 cells/well. After 24 h, cells were subjected to serum-depleted media for 4 h prior to treatment with *T. rubra* inflorescence, bract, and flower extracts for 16 h. Following the incubation period, cells were collected, fixed with a 4% ethanol solution, and the cell cycle analysis protocol was applied by incubating samples in a mixture of 0.1% (v/v) triton X-100, 0.5 mg/mL RNaseA, and 5 µg/mL PI solution. 20.000 events were analyzed by Guava easyCyte Flow Cytometer (Merck Millipore, Germany).

Cell death analysis by annexin V assay

The relative percentage of apoptotic MIA PaCa-2 cells in response to *T. rubra* inflorescence, bract, and flower extracts was analyzed by the Annexin V-FITC apoptosis detection assay according to the manufacturer's protocol (Annexin V-FITC Reagent, Elabscience). 3×10^5 cells/well seeded on 6-well plates were treated with 10 µM DOX as a positive control and *T. rubra* inflorescence, bract, and flower extracts for 16 h. After the completion of the incubation period, the media of the cells for each condition were collected, and the wells were washed with

1X PBS. The attached cells were then collected with 0.25% trypsin-EDTA, and the whole suspension of cells was centrifuged at 350xg for 5 min. 1×10^6 cells from each sample were treated with Annexin Binding Buffer, Annexin V, and PI according to the manufacturer's protocol. 20.000 events were analyzed immediately by Guava easyCyte Flow Cytometer (Merck Millipore, Germany).

Chemometrics analysis

17 different analyses were performed on 4 different plant species. An excel sheet were generated for chemometric analysis. An unsupervised (Principal Component Analysis) and a supervised (Partial Least Square- Discriminant Analysis) models were applied to data set. In order to perform this models, 4 groups were generated for Y-Block and 17 parameters were transferred into X-Block. Data were transferred into MATLAB 2023b software. Data cleaning, outlier detection and data normalization were applied. After all, data matrices were transferred into PLS Toolbox 9.5.0 for chemometric analysis. 17×36 data matrices were evaluated for classification and feature selection. PCA analysis were shown the discrimination between the species and PLS-DA analysis were performed to indicate the statistically significant parameters which are differentiated between the groups. A correlation map was also plotted in order to elucidate the relation between the parameters. A heatmap was also generated to monitor the whole differences and similarities of each sample regarding to different analysis.

Statistical analysis

All repeated experiments were conducted in triplicate. Statistical analyses were performed using GraphPad Prism 8 (GraphPad Software, Inc., San Diego, CA; Version 8.4.3) and Excel. Differences between groups were determined using one-way ANOVA followed by Tukey's post-hoc tests. Correlations of the parameters were evaluated using Spearman's correlation test. The differences were considered significant at $p < 0.05$.

Results

Phytochemical characterization and quantification of the marker components of *Tilia* species by HPTLC and HPLC

The chemical profiles of hydroethanolic extracts of different parts of four *Tilia* species were analyzed by HPTLC (Fig. 1). The flowers and bracts of *Tilia* species showed characteristic chemical fingerprints. Detailed information regarding the retardation factors (R_F) of standards can be found in Supplementary Table S4.

According to the HPTLC profiles, most of the investigated standards as protocatechuic acid, tiliroside, quercitrin, astragalin, isoquercitrin, and hyperoside were identified in the samples. Apart from the investigated compounds as distinct yellow- and blue-colored zones, with R_F values of approximately 0.5 and 0.75, respectively, were observed in *T. rubra* bracts. These zones represent unknown compounds that require further investigation for identification.

In addition to the qualitative analysis of *Tilia* species, quantitative analysis was also performed on the investigated compounds. The calculated values are given in Table 1. The highest amounts of protocatechuic acid and hyperoside were found in the bracts of *T. cordata* and *T. rubra* at 30 mg/g and 3 mg/g, respectively. The highest amounts of isoquercitrin (15 mg/g) and astragalin (9 mg/g) were quantified in the flowers of *T. cordata* and *T. tomentosa*, respectively. All samples except the bracts of *T. rubra* contained tiliroside; however, the bracts of *T. rubra* were found to have the highest quercitrin content at 23 mg/g.

TPC, TFC, and antioxidant activity of the extracts

The highest phenolic content was determined in *T. rubra* flowers, followed by *T. rubra* bracts and *T. rubra* inflorescence (Table 2). Additionally, the highest flavonoid content was determined in *T. rubra* bracts.

The hydroethanolic extracts of bracts belonging to *T. rubra*, which had the highest TFC values, also showed potent antioxidant activity with DPPH, FRAP, and CUPRAC assays.

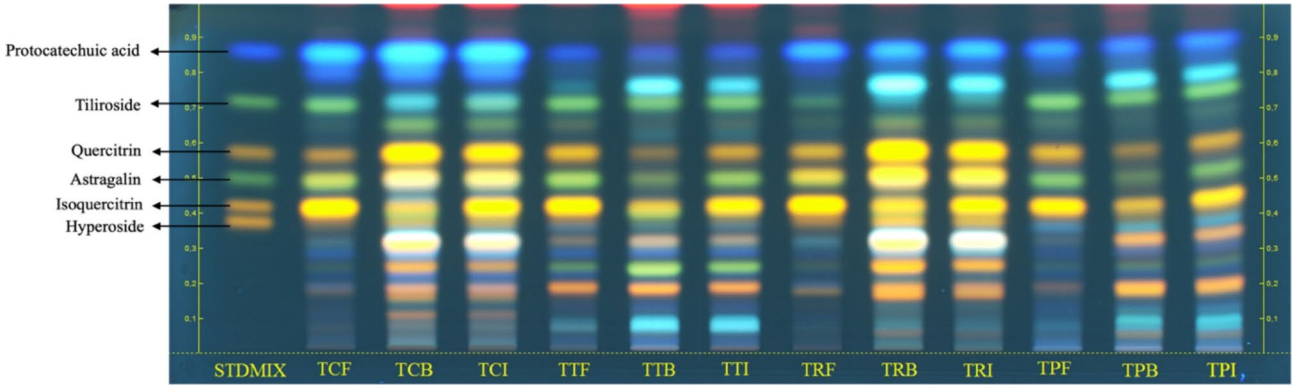

Fig. 1. HPTLC chromatogram of flower, bract, and inflorescence extracts of *T. cordata* (TC), *T. tomentosa* (TT), *T. rubra* (TR), and *T. platyphyllos* (TP). F: Flowers; B: Bracts; I: Inflorescence.

Samples		Investigated compounds (mg/g extract)					
		Protocatechuic acid	Hyperoside	Isoquercitrin	Astragalin	Quercitrin	Tiliroside
T. cordata	Flowers	13.35 ± 0.41	n.d.	15.06 ± 0.34	7.76 ± 0.12	1.71 ± 0.04	4.78 ± 0.05
	Bracts	30.26 ± 0.82	1.74 ± 0.03	n.d.	2.12 ± 0.05	17.87 ± 0.21	0.24 ± 0.02
	Inflorescence	28.85 ± 0.27	1.47 ± 0.01	14.82 ± 0.09	6.94 ± 0.08	11.68 ± 0.10	3.1 ± 0.06
T. platyphyllos	Flowers	3.12 ± 0.10	n.d.	7.24 ± 0.15	6.40 ± 0.05	3.43 ± 0.03	5.57 ± 0.06
	Bracts	2.03 ± 0.06	n.d.	2.12 ± 0.03	1.37 ± 0.004	1.07 ± 0.01	3.12 ± 0.05
	Inflorescence	2.68 ± 0.09	n.d.	5.41 ± 0.10	3.74 ± 0.03	2.32 ± 0.02	4.36 ± 0.06
T. rubra	Flowers	6.19 ± 0.01	n.d.	13.43 ± 0.03	4.85 ± 0.02	2.51 ± 0.02	0.90 ± 0.03
	Bracts	6.68 ± 0.17*	3.01 ± 0.04	4.44 ± 0.11	1.73 ± 0.04	23.13 ± 0.33	n.d.
	Inflorescence	7.46 ± 0.51*	2.28 ± 0.02	10.16 ± 0.17	3.64 ± 0.05	13.67 ± 0.19	0.59 ± 0.01
T. tomentosa	Flowers	1.18 ± 0.03	n.d.	11.02 ± 0.22	8.89 ± 0.09	3.43 ± 0.02	4.30 ± 0.65
	Bracts	1.15 ± 0.01*	n.d.	2.20 ± 0.05	1.77 ± 0.02	0.83 ± 0.01	3.23 ± 0.02
	Inflorescence	0.99 ± 0.04*	n.d.	7.24 ± 0.15	5.81 ± 0.06	2.27 ± 0.03	4.18 ± 0.03

Table 1. Quantitative results of compounds in *Tilia* species investigated by HPLC. The quantified investigated standards were expressed as mg in hydroethanolic extract (g) of *Tilia* species; $n = 3$. n.d.: not detected. *Co-eluted with an unknown compound.

Samples		TPC (mg GAE/g)	TFC (mg QE/g)	DPPH (mg TE/g)	FRAP (mg TE/g)	CUPRAC (mg TE/g)
T. cordata	Flowers	237.93 ± 9.03	21.26 ± 0.60	556.27 ± 22.44	302.66 ± 8.57	787.79 ± 78.08
	Bracts	223.03 ± 3.18	45.67 ± 1.53	518.59 ± 14.55	263.72 ± 20.62	768.38 ± 26.23
	Inflorescence	245.32 ± 13.20	34.33 ± 3.60	558.34 ± 12.67	277.13 ± 8.84	806.72 ± 36.66
T. platyphyllos	Flowers	128.48 ± 8.14	15.38 ± 0.26	165.38 ± 8.41	127.03 ± 17.18	425.55 ± 12.64
	Bracts	57.92 ± 9.12	27.17 ± 1.92	144.90 ± 4.55	70.74 ± 2.84	197.89 ± 21.79
	Inflorescence	153.18 ± 2.79	23.70 ± 0.71	312.35 ± 6.37	183.29 ± 5.12	558.24 ± 60.96
T. rubra	Flowers	336.31 ± 19.89	19.64 ± 1.10	561.45 ± 19.88	446.05 ± 5.88	693.15 ± 22.59
	Bracts	307.50 ± 11.64	58.61 ± 2.85	727.17 ± 2.11	374.20 ± 7.64	203.36 ± 18.84
	Inflorescence	295.43 ± 8.87	36.67 ± 2.22	638.44 ± 14.39	340.85 ± 17.77	487.81 ± 47.37
T. tomentosa	Flowers	232.68 ± 11.29	18.93 ± 0.79	495.27 ± 22.69	86.54 ± 14.74	693.15 ± 22.59
	Bracts	56.55 ± 3.67	24.31 ± 2.80	53.92 ± 10.01	32.75 ± 4.12	203.36 ± 18.84
	Inflorescence	165.63 ± 12.12	22.32 ± 0.82	270.88 ± 16.20	90.08 ± 7.16	487.81 ± 47.37

Table 2. TPC, TFC, and antioxidant activity results of the *Tilia* samples. *TPC* Total phenolic content; *TFC* Total flavonoid content; *DPPH* DPPH radical scavenging activity; *FRAP* Ferric reducing antioxidant power; *CUPRAC* Copper reducing antioxidant capacity.

Cell culture studies

Evaluation of inflammatory response

The inflammation parameters were evaluated for the concentrations at which the extracts yielded a viability above 70% in the RAW264.7 cell viability assay (Table 3).

– **Nitrite inhibition**

According to the results, 2 h of pre-treatment with *Tilia* samples showed significant reducing effects on nitrite levels compared with 100 µM indomethacin. According to the comparative evaluation of different *Tilia* species extracts, all extracts effectively reduced inflammation by preventing nitric oxide (NO) generation dose-dependently (Table 3). The percentage of nitrite inhibition was over 50% for all non-cytotoxic concentrations (0.125–1 mg/mL).

– **IL-6 and PGE_2releasing ınhibition**

According to the findings, *T. rubra* flowers at a 0.5 mg/mL concentration exerted the highest inhibitory activity against LPS-activated release of IL-6 (Table 3).

As per our results, *T. rubra* inflorescence at a concentration of 0.5 mg/mL exerted the highest inhibitory activity against PGE_2 production, followed by *T. platyphyllos* bracts at the same concentration. The minimum inhibitory effect was obtained for *T. cordata* bracts at 1 mg/mL concentration, followed by *T. tomentosa* inflorescence at the same concentration (Table 3).

Groups	Concentration (mg/mL)	Cell viability (%)	Nitrite (μM)	Nitrite inhibition (%)	IL-6[A] (pg/mL)	PGE_2[A] (pg/mL)
Control	–	124.99 ± 1.94	1.31 ± 0.52	–	313.38 ± 0.42	13.55 ± 2.78
Control + LPS	–	100.00 ± 0.52	33.04 ± 1.12	–	5817.03 ± 460.80	269.10 ± 18.94
Indomethacin	100 μM	98.57 ± 1.46	16.40 ± 1.52*	50.36 ± 4.42	2499.47 ± 338.26*	25.09 ± 3.64*
L-name	100 μM	98.05 ± 1.42	19.67 ± 0.79*	40.43 ± 2.76	3899.16 ± 574.38*	27.79 ± 8.15*
T. cordata flowers	0.125	98.51 ± 0.67	14.56 ± 0.53*	55.80 ± 2.23		
	0.25	98.77 ± 1.75	14.43 ± 1.33*	56.23 ± 4.82		
	0.5	90.39 ± 0.24	10.95 ± 1.46*	66.77 ± 5.90		
	1	84.67 ± 2.59	4.67 ± 0.74*	85.87 ± 2.94	582.98 ± 108.23*	73.71 ± 19.84*
T. cordata bracts	0.125	97.39 ± 3.20	12.20 ± 1.66*	62.96 ± 0.50		
	0.25	93.95 ± 0.81	11.60 ± 1.22*	64.78 ± 0.48		
	0.5	81.32 ± 0.46	8.55 ± 1.20*	74.08 ± 3.56		
	1	74.43 ± 2.26	5.13 ± 0.88*	84.50 ± 4.31	516.15 ± 32.58*	236.35 ± 32.11
T. cordata inflorescence	0.125	94.41 ± 0.10	13.96 ± 1.43*	57.62 ± 1.25		
	0.25	87.68 ± 0.92	13.64 ± 0.78*	58.60 ± 0.66		
	0.5	84.63 ± 0.10	11.65 ± 1.53*	64.66 ± 2.28		
	1	80.07 ± 2.96	4.52 ± 0.87*	86.33 ± 1.47	522.60 ± 10.54*	136.98 ± 10.89*
T. platyphyllos flowers	0.125	95.85 ± 0.33	16.28 ± 0.95*	50.59 ± 0.40		
	0.25	89.54 ± 1.12	13.78 ± 1.42*	58.20 ± 2.44		
	0.5	87.19 ± 0.39	8.82 ± 1.63*	73.23 ± 4.76		
	1	82.48 ± 3.05	4.76 ± 2.02*	85.76 ± 2.15	597.3 ± 6 32.90*	52.92 ± 0.08*
T. platyphyllos bracts	0.125	89.24 ± 3.11	11.46 ± 1.34*	67.27 ± 1.12		
	0.25	83.91 ± 1.48	9.24 ± 2.03*	71.79 ± 1.98	695.41 ± 36.44*	33.91 ± 0.31*
	0.5	64.90 ± 2.17	–	–		
	1	62.45 ± 0.37	–	–		
T. platyphyllos inflorescence	0.125	92.55 ± 0.33	14.10 ± 1.50*	57.20 ± 0.14		
	0.25	81.65 ± 4.23	10.17 ± 1.76*	58.88 ± 0.92		
	0.5	74.12 ± 0.14	9.06 ± 1.27*	72.54 ± 2.73	467.24 ± 12.70*	40.41 ± 12.01*
	1	65.07 ± 1.16	–	–		
T. rubra flowers	0.125	89.43 ± 3.42	11.56 ± 0.37*	64.94 ± 2.89		
	0.25	89.22 ± 0.72	10.86 ± 2.93*	67.06 ± 3.69		
	0.5	73.74 ± 0.57	8.82 ± 1.54*	73.23 ± 9.96	310.53 ± 12.10*	58.82 ± 5.37*
	1	67.19 ± 3.28	–	–		
T. rubra bracts	0.125	96.22 ± 1.02	14.06 ± 0.46*	57.36 ± 4.21		
	0.25	90.63 ± 1.01	12.20 ± 1.80*	62.96 ± 0.90		
	0.5	89.40 ± 2.63	11.28 ± 0.25*	65.78 ± 2.51	2885.66 ± 101.15*	45.49 ± 7.42*
	1	58.60 ± 4.11	–	–		
T. rubra inflorescence	0.125	98.79 ± 1.61	12.48 ± 2.33*	62.13 ± 2.87		
	0.25	96.45 ± 2.35	11.83 ± 2.45*	64.10 ± 4.88		
	0.5	82.60 ± 1.49	6.69 ± 1.67*	79.69 ± 3.22	583.18 ± 131.34*	30.99 ± 6.36*
	1	64.69 ± 3.91	–	–		
T. tomentosa flowers	0.125	101.39 ± 2.74	13.36 ± 1.32*	59.51 ± 1.54		
	0.25	84.29 ± 3.10	11.23 ± 0.79*	65.95 ± 1.26		
	0.5	81.27 ± 1.28	10.56 ± 0.66*	68.94 ± 2.84		
	1	71.35 ± 3.60	3.87 ± 1.22*	88.29 ± 1.88	500.33 ± 83.00*	84.56 ± 12.26*

Continued

Groups	Concentration (mg/mL)	Cell viability (%)	Nitrite (μM)	Nitrite inhibition (%)	IL-6[A] (pg/mL)	PGE_2[A] (pg/mL)
T. tomentosa bracts	0.125	100.81 ± 2.01	7.67 ± 1.02*	84.03 ± 0.52		
	0.25	85.99 ± 2.46	4.24 ± 1.77*	88.95 ± 2.27		
	0.5	73.50 ± 4.507	3.96 ± 0.65*	89.10 ± 0.71		
	1	71.13 ± 1.81	3.29 ± 0.87*	90.11 ± 1.65	452.69 ± 1.22*	71.16 ± 9.99*
T. tomentosa inflorescence	0.125	98.85 ± 5.47	12.94 ± 1.65*	60.72 ± 1.68		
	0.25	92.32 ± 0.28	12.20 ± 1.80*	62.97 ± 2.09		
	0.5	90.33 ± 0.96	11.46 ± 2.01*	65.22 ± 1.49		
	1	84.62 ± 1.99	3.55 ± 0.43*	89.26 ± 2.10	1806.48 ± 277.63*	143.39 ± 12.28

Table 3. The effects of *Tilia* sp. on LPS-induced NO, IL-6, and PGE_2 production in RAW264.7 cells. [A]The parameters IL-6 and PGE_2 were tested at the highest non-cytotoxic dose of the extracts. *Ctrl* Control group treated with DMEM; *Ctrl + LPS* Control group only stimulated with LPS; *IND* Indomethacin (100 μM); *L-NAME* N G-nitro-L-arginine methyl ester hydrochloride (100 μM). Results were expressed as mean ± SD compared with control. The significant differences between groups and Ctrl + LPS were denoted with $^*p < 0.05$. *LPS* Lipopolysaccharides from *E. coli*; *L-NAME* Nv-Nitro-L-arginine methyl ester hydrochloride; *IND* Indomethacin. *IL-6* interleukin-6.

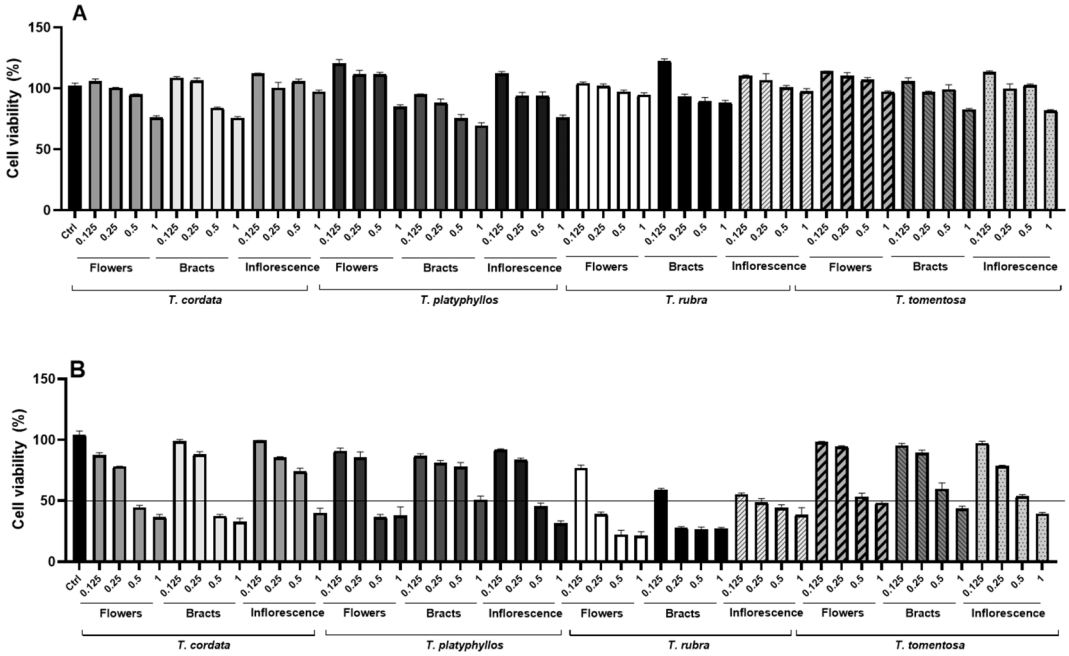

Fig. 2. Effects of *Tilia* species on the viability of HDF (**A**) and MIA PaCa-2 (**B**) cells.

Anticancer activity

Two-dimensional cell cytotoxicity

All extracts exerted selective cytotoxic activity against MIA PaCa-2 cells, while at least 70% cell viability was obtained with normal human dermal cells (Fig. 2). All extracts showed potent anticancer activity in a dose-dependent manner against pancreatic cells, decreasing cell viability by at least 50% at a concentration of 1 mg/mL. *T. rubra* bracts exerted the highest cytotoxic activity on MIA PaCa-2 cells at the highest concentration with an IC_{50} of 0.16 ± 0.01 mg/mL followed by *T. rubra* flowers (IC_{50} = 0.21 ± 0.01 mg/mL) and inflorescence (IC_{50} = 0.24 ± 0.05 mg/mL) (Supplementary Table S5).

A strong negative correlation was detected between hyperoside and quercitrin with IC_{50} level (mg/mL) for Mia PACA-2 cell line (r = – 0.914, $p < 0.0001$, r = – 0.479, $p = 0.0031$ respectively). Moreover, a significant negative correlation was found between TPC and both MIA PaCa-2 cell viability (r = – 0.516, $p = 0.01$) and the IC_{50} value for cell viability (r = – 0.593, $p = 0.0001$).

Three-dimensional spheroid formation/growth

T. rubra extracts from different parts caused a significant reduction in the growth rate of the spheroids obtained, while the control spheroids-maintained growth for up to 9 days. Even at the lowest dose (0.125 mg/mL), all investigated parts of *T. rubra* reduced the growth rate of spheroids compared with the control. At the highest

dose (1 mg/mL), bracts of *T. rubra* showed the most substantial spheroid size change (50% reduction). The changes in spheroid diameters of MIA-PaCa-2 cells treated with extracts from flowers, bracts, and inflorescences of *T. rubra* are provided in Supplementary Table S6. DOX as a reference molecule slowed spheroid growth by 70% compared with the control after 9 days of treatment at a 10 µM concentration. Figure 3 shows spheroid images taken every 3 days.

As inflorescences of *Tilia* species are traditionally used, extracts at the highest doses (1 mg/mL) were further investigated with a 3D spheroid growth assay. The variations in spheroid diameters of cells are outlined in Supplementary Table S7. All species reduced the growth rate of spheroids compared with the control. Similar to our results obtained by the 2D cell cytotoxicity assay, at a 1 mg/mL dose, *T. rubra* showed the highest anticancer activity, with a 50% reduction in size, followed by *T. cordata* (32%) and *T. tomentosa* (24%).

According to the 2D cytotoxicity assay and 3D spheroid growth assay results, all parts of *T. rubra* (1 mg/mL) were further investigated for apoptosis and necrosis profiles.

The effect of plant derivatives on cell cycle progression of MIA PaCa-2 cells

In order to demonstrate the effect of *T. rubra* inflorescence, bract, and flower extracts on cell cycle arrest, MIA PaCa-2 cells were treated with 1 mg/mL of extracts from each part for 24 h. (Fig. 4). The average G0/G1 cell population among non-treated, *T. rubra* inflorescence-treated, bract-treated, and flower-treated cells was 68.45%, 86.94%, 92.25%, and 79.38%, respectively. The average percentage of cells in the S phase for non-treated MIA PaCa-2 cells was 6.13%, while *T. rubra* inflorescence, bract, and flower extract-treated cell percentages were found to be 6.13%, 5.91%, and 9.93%, respectively. The population of cells in G2/M phase was 7.32%, 1.98%, and 11.0% after treatments with *T. rubra* inflorescence, bract, and flower in a respective order. For the control group, the frequency of the G2/M cell cycle phase was found to be 15.77%.

In vitro anti-cancer activity of plant derivatives on MIA PaCa-2 cells

MIA PaCa-2 cells were treated with 1 mg/mL of *T. rubra* inflorescence, bract, and flower extracts, along with 10 µM of DOX as a positive control, for 24 h. Cell death was measured using a flow cytometry method employing an Annexin V-FITC/PI apoptosis assay detection kit. The results revealed minimal apoptotic and necrotic cells in the control group (Fig. 5). In contrast, cells treated with 10 µM DOX, a cell death inducer, exhibited 65% necrosis. Similarly, *T. rubra* inflorescence, bract, and flower extract treatments led to an increase in necrotic cell percentages. Treatment with 1 mg/mL of *T. rubra* inflorescence resulted in 60.84% necrotic cells stained with PI and 4.16% Annexin-V-stained apoptotic cells. Likewise, bract and flower treatments showed 54.39% and 66.53% PI-stained necrotic cells and 3.80% and 5.21% Annexin-V-stained apoptotic cells, respectively, after 24 h. Overall, *T. rubra* inflorescence, bracts and flowers induced statistically similar levels of necrotic cell death at 24 h.

Chemometric analysis

Data matrices were generated in order to monitor the alteration of different species in accordance with our experimental findings. A multivariate data analysis was performed via 18 × 36 data matrices including flowers, bracts and inflorescence of 4 different plat species (cordata, rubra etc.) (Fig. 6). Principal component analysis was carried out and specificity and sensitivity were found to be better than 1.00 (for each group) and 0.889 (the worse value for cordata), respectively. Root Mean Square of Calibration (RMSEC) value were calculated to be 0.53 while Root Mean Square Error of Cross Validation (RMSECV) values were 0.69. Three components were selected to explain model 54.64% of variance for X block and 83.99% of variance for Y block were captured by the PCA model. A PLS-DA analysis was also performed for feature selection and VIP scores were monitored in Fig. 7 which elucidated the significant alterations between the groups. PLS-DA analysis was also indicated that groups were significantly separated. ROC curves for each species were plotted and provided in Supplementary Fig. 1. The correlation between the parameters were emphasized via correlation map by PLS Toolbox for MATLAB software (Supplementary Fig. 2). A heat map was also plotted in order to summarize all findings. In order to

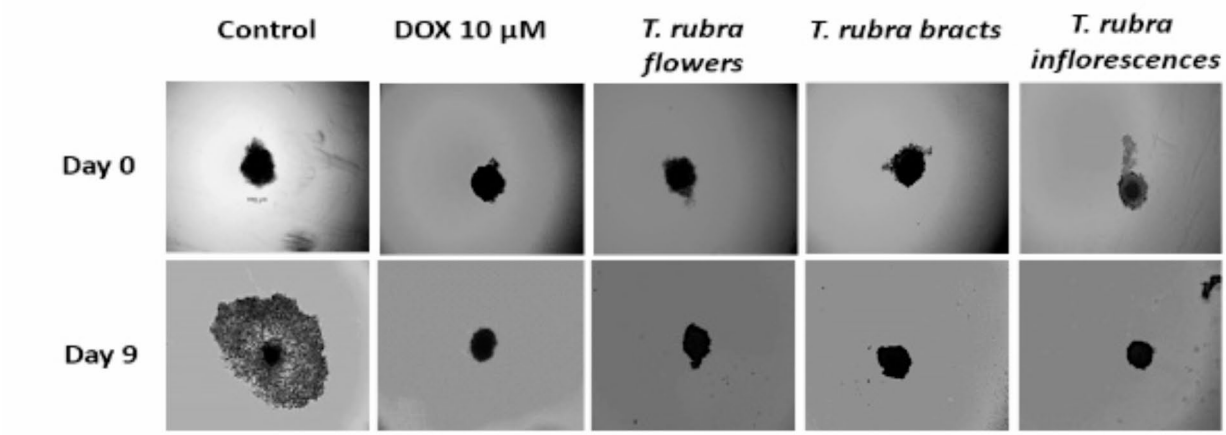

Fig. 3. Images of Mia PACA-2 tumor spheroids at the beginning (Day 0) and the end (Day 9) of the experiment (after incubation with 1 mg/mL of the different parts of *T. rubra* extract). Magnification rate: 10X.

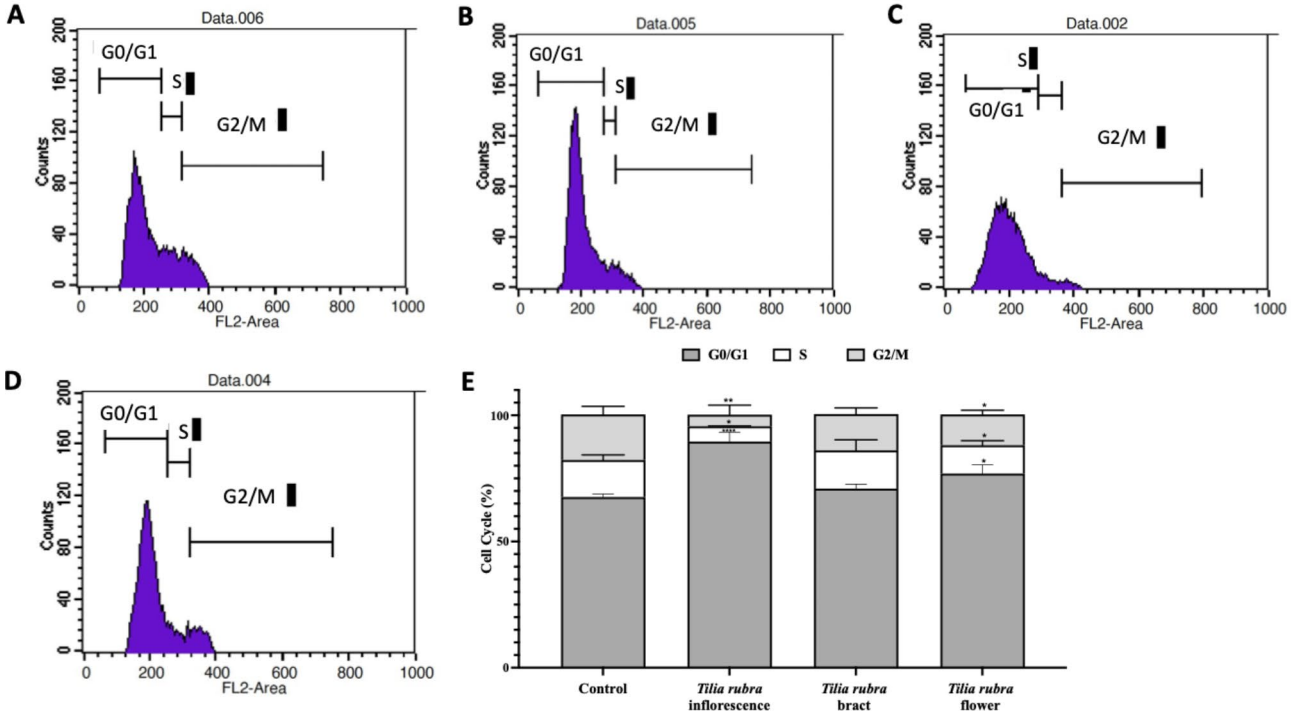

Fig. 4. Cell cycle profiles of MIA PaCa-2 cells examined by flow cytometry. (**A**) Control MIA PaCa-1 cells, (**B**) 1 mg/mL of *T. rubra* inflorescence treated MIA PaCa-2 cells, (**C**) 1 mg/mL of *T. rubra* bract treated MIA PaCa-2 cells (**D**) 1 mg/mL of *T. rubra* flower-treated MIA PaCa-2 cells and (**E**) overall cell cycle profiles after treatment with plant derivatives. (****$p \leq 0.001$).

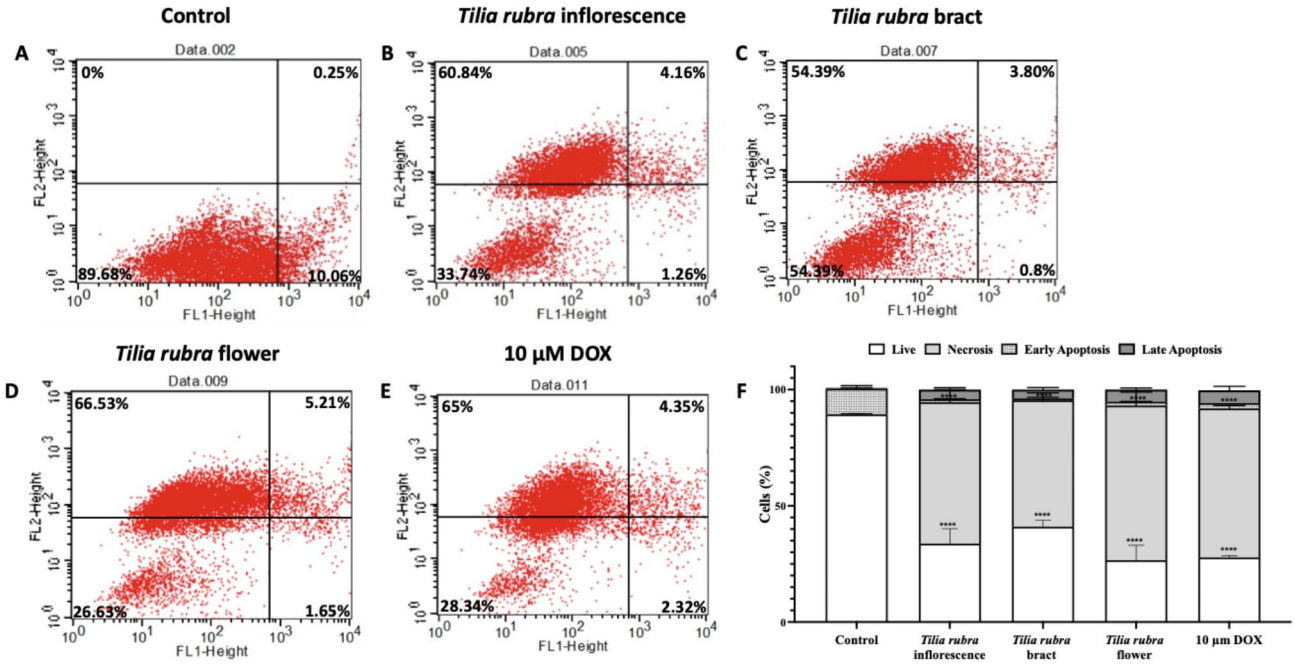

Fig. 5. Effect of *T. rubra* inflorescence, bract, and flower extracts on the pancreatic carcinoma cell line, MIA PaCa-2, following 24-h treatment. (**A**) Non-treated MIA PaCa-2 cells, (**B**) MIA PaCa-2 cells treated with 1 mg/mL *T. rubra* inflorescence, (**C**) 1 mg/mL *T. rubra* bract, and (**D**) 1 mg/mL *T. rubra* flower were subjected to both Annexin V-FITC and propidium iodide prior to analysis using flow cytometry. (**E**) Doxorubicin (10 µM) was used as a positive control. Dot plot representing control and plant-derivative treated cells. (**F**) The scatter plot represents the percentages of necrosis (upper left), late apoptosis (upper right), viable cells (lower left), and early apoptosis (lower right) populations of MIA PaCa-2 cells in respective order. (****$P \leq 0.001$).

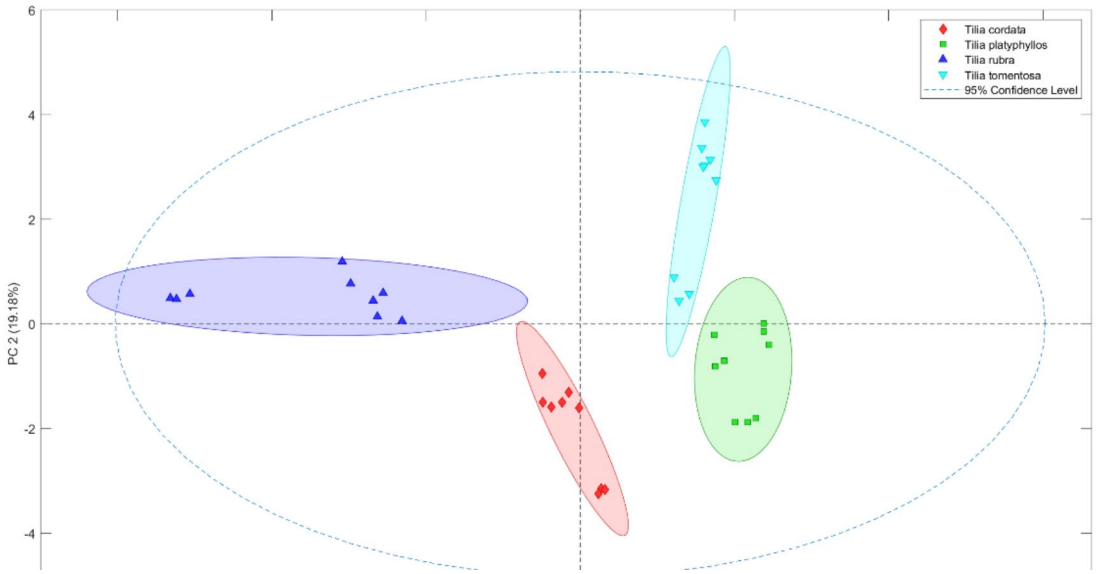

Fig. 6. Score plot for 4 different species (*T. cordata*, *T. platyphyllos*, *T. rubra*, *T. tomentosa*).

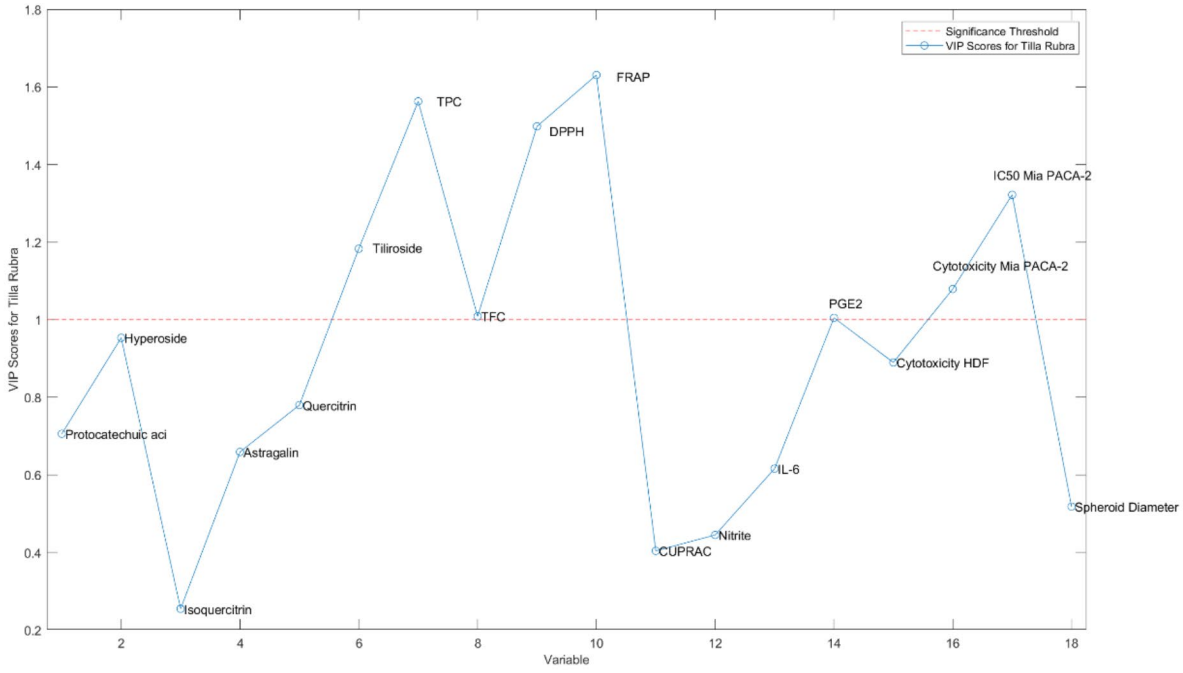

Fig. 7. PLS-DA Variable in Projection scores for each parameter for *T. rubra*. Parameters has greater value than the threshold (1.0) accepted to be significantly altered.

perform such analysis, all parameters were scaled by calculating z-score and new data matrices were generated via MATLAB 2023b software (Fig. 8).

According to VIP scores and Heatmap illustrations; Tiliroside, TPC, TFC, DPPH, FRAP, cytotoxicity against Mia PACA-2 cell line and IC_{50} values were passed the significant threshold. These parameters were found to be statistically significant for *T. rubra* species against the others.

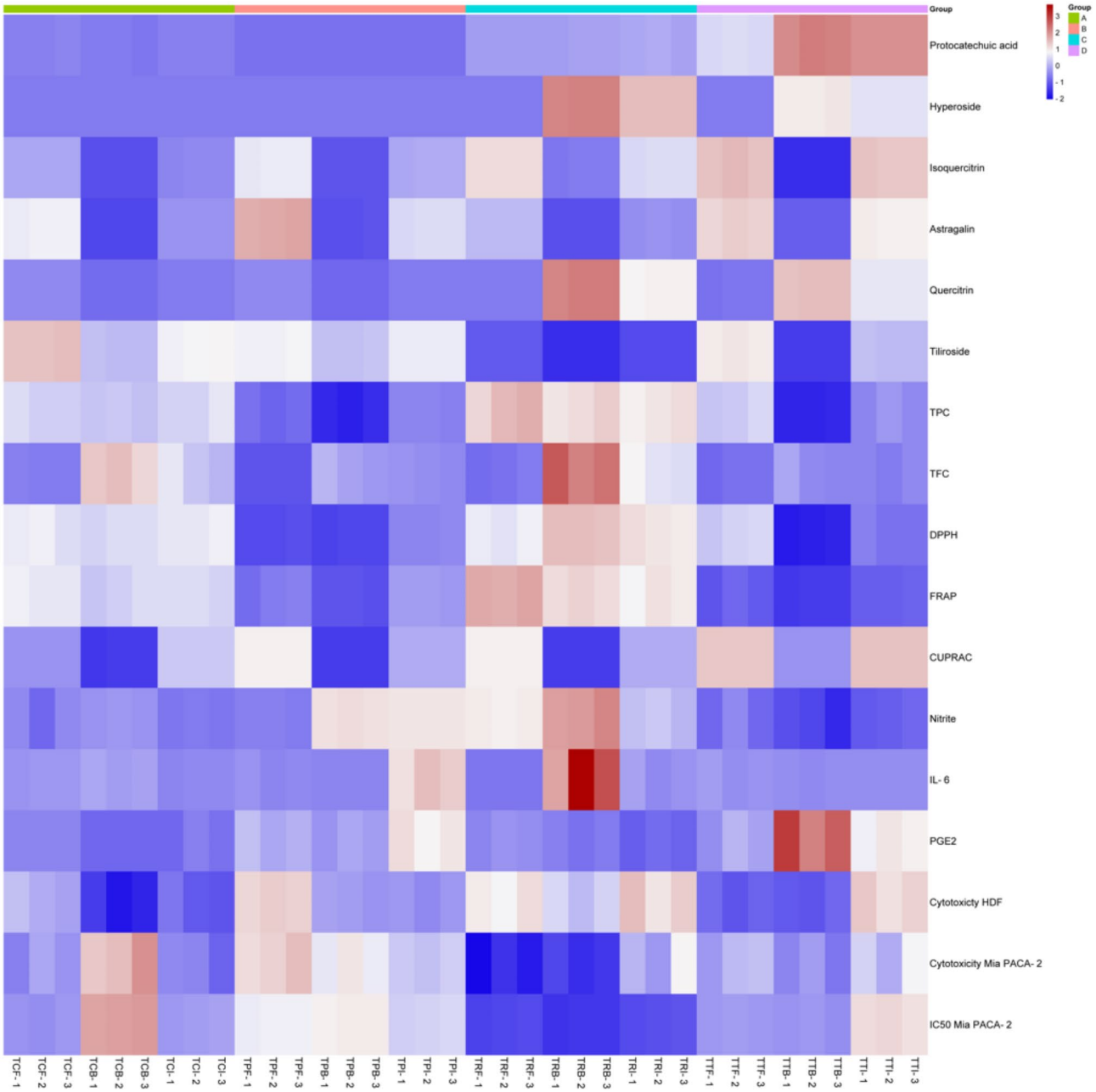

Fig. 8. Heatmap for 4 different species *T. cordata* (**A**), *T. platyphyllos* (**B**), *T. rubra* (**C**), *T. tomentosa* (**D**).

Discussion

This study investigated the anti-cancer potentials of hydroethanolic *Tilia* species extracts from different plant parts against MIA PaCa-2 pancreatic cancer cells, as well as the underlying cancer-triggering mechanisms.

Oxidative stress and chronic inflammation are involved in all stages of cancer. ROS may directly damage DNA by introducing structural alterations and gene mutations into the DNA in the initiation stage; block cell-to-cell communication, induce abnormal gene expression, and modify secondary messengers in the promotion stage; and eventually cause an increase in cell proliferation and a decrease in apoptosis. While ROS produced as a part of the inflammatory response facilitates the clearance of pathogens, when produced in excessive amounts and for prolonged periods, it leads to oxidative stress and diseases associated with chronic inflammation[1,2]. Therefore, we analyzed the chemical components indicating antioxidant and anti-inflammatory characteristics.

Phenolic compounds are the biggest phytochemical group and have drawn increasing interest due to their ability to prevent and treat oxidative stress-related diseases by inhibiting oxidative damage to proteins, DNA, and lipids, which may lead to mutation, apoptosis, and carcinogenesis[30]. Toker et al. (2001) found quercetin 3,7-dirhamnoside, quercitrin, astragalin, isoquercitrin, and rutin to be the main and common compounds among the *Tilia* species *T. platyphyllos*, *T. rubra*, and *T. tomentosa*[31]. Ziaja et al. (2020) investigated the flavonoids

in flowers of *T. cordata*, *T. platyphyllos*, *T.* x *vulgaris*, *T. tomentosa*, and *T. americana*, revealing isoquercitrin, astragalin, tiliroside, and protocatechuic acid as the common compounds among them[32]. These compounds of *Tilia* species can exhibit a wide range of biological activities, including antioxidant, anti-inflammatory, and anticancer properties[6,11,33–35]. In this study, we characterized *Tilia* species in terms of the amounts of protocatechuic acid, hyperoside, isoquercitrin, astragalin, quercitrin, and tiliroside and investigated their contributions to the pharmacological activity. We found that hyperoside and quercitrin levels as well as TPC were strongly correlated with reduced IC_{50} values in Mia PACA-2 cells. However, since hyperoside was not detected in all extracts, we attributed the observed effects to quercitrin. It should be noted that other compounds detected in *Tilia* species might have contributed to the pharmacological activity since the extract constituents might exhibit additive or synergistic effects.

Free radical scavenging activities of flavonoids have been attributed to their ability to donate hydrogen from their phenolic hydroxyl groups, stabilizing free radicals[36]. Accordingly, the hydroethanolic *T. rubra* bract and flower extracts, which had the highest TFC and TPC values, respectively, showed potent antioxidant activity.

Macrophages play a crucial role in the immune system by mediating inflammation and initiating defense mechanisms. When stimulated, RAW 264.7 macrophages produce a variety of pro-inflammatory mediators, such as NO and interleukins, making them an ideal model for assessing the anti-inflammatory and immunomodulatory properties of any compound[37]. Our results showed that all extracts effectively and dose-dependently reduced LPS-induced inflammation in RAW 264.7 cells by preventing NO generation. Toker et al. (2004) reported that 50 mg/kg of *T. tomentosa* leaves inhibited inflammation in a paw edema model stimulated with carrageenan[38]. Similarly, *T. tomentosa* extracts inhibited nitrite production by 89–90%, providing potent protection against inflammation. Moreover, Fawzy et al. (2018) reported that a 70% methanolic extract of *T. cordata* aerial parts exerted anti-inflammatory activity against carrageenan-induced rat paw edema test equal to indomethacin at a 300 mg/kg dose[39]. Jabeur et al. (2017) from Portugal reported that 0.2 mg/mL of hydroethanolic *T. platyphyllos* aerial part extract inhibits NO production by 50% in RAW264.7 cells[13]. In line with these findings, in our study, all extracts showed more than 50% inhibition even at 125 µg/mL, the lowest dose tested.

Supporting the anti-inflammatory activities of *Tilia* species, LPS-activated release of IL-6, an important pro-inflammatory cytokine, was inhibited in this study, with *T. rubra* flowers exerting the highest inhibitory activity. Moreover, the inflorescence extract was the most potent in reducing the release of PGE_2, which occurs following a harmful stimulus and results in localized edema[40].

The anticancer activities of *Tilia* extracts were assessed by HDF and MIA PaCa-2 cell monolayers prior to the 3D spheroid model. The cytotoxic effects of *Tilia* extracts on normal and cancer cells vastly differed in that potent anticancer activity was observed against MIA PaCa-2 pancreatic cancer cells, while no toxicity was exerted on HDF cells. Further, *T. rubra* extracts exerted the highest cytotoxic activity. In line with our findings, Barreiro et al. (2006) demonstrated that exposure to *T. cordata* flower extracts resulted in a selective and dose-dependent antiproliferative effect on tumoral BW 5147 lymphocytes, leading to apoptosis[15]. In normal lymphocytes, all extracts suppressed mitogen-induced proliferation. Jabeur et al. (2017) demonstrated the antitumor activity of a 70% ethanolic extract of *T. platyphyllos* aerial parts on HeLa cervix cancer, HepG2 hepatocellular carcinoma, NCI-H460 lung carcinoma, and MCF-7 breast adenocarcinoma cells[13]. *T. tomentosa* extracts prepared using an ethanol/ethyl acetate/water mixture also showed a selective effect on A549 lung adenocarcinoma cells compared with nonmalignant HaCaT cells[16].

This is the first study to demonstrate the anticancer effect of *T. rubra*. Moreover, the anticancer activity of *Tilia* species on 3D spheroid growth was evaluated for the first time, which is crucial since 3D models more closely resemble the conditions in the microenvironment than 2D models. While we assessed the anti-cancer activities of different *Tilia* species, since all parts of *T. rubra* showed more potent anticancer activity than other extracts in the 2D cytotoxicity assay, only *T. rubra* extracts were included in the spheroid growth assay.

Extracts from various parts of *T. rubra* led to a significant reduction in spheroid growth even at the lowest dose tested. This is in line with a previous finding, where plant-based compounds demonstrated an ability to inhibit cancer cell proliferation in both 2D and 3D models[41]. Other studies have reported that natural compounds induce cell cycle arrest, consequently inhibiting cancer progression[42,43]. Here, we report a similar mechanism, where *T. rubra* inflorescence, bract, and flower extracts trigger the activation of different checkpoints in the cell cycle, further supporting the notion that plant-derived compounds can interfere with critical regulatory points in cancer cell proliferation[44].

Given that both cytotoxicity and spheroid assays confirmed the notable effects of *T. rubra* extracts, their apoptotic and necrotic potential was further investigated. Consistent with findings from earlier research, where necrosis was identified as a key pathway in plant extract-induced cytotoxicity[45], cells treated with the *T. rubra* flower extract exhibited the highest necrotic population. Furthermore, both *T. rubra* inflorescence and bract extracts induced similar levels of necrotic cell death within 24 h of treatment, suggesting that plant extracts from various parts contribute similarly to the induction of necrosis. The ability of *T. rubra* extracts to arrest the cell cycle and induce necrosis presents a compelling case for its potential as an anticancer agent[46]. Taken together, results from cytotoxicity assays, spheroid growth inhibition, and cell death analyses provide a robust foundation for further investigation into the molecular mechanisms underlying the anticancer properties of *T. rubra*. In addition, according chemometric analysis, tiliroside, TPC, TFC, DPPH, FRAP, cytotoxicity against Mia PACA-2 and IC_{50} parameters were passed the significant threshold. These parameters were found to be statistically significant for *T. rubra* species against the others. These findings suggest that antioxidant capacity and cytotoxicity of *T. rubra* species were significantly altered compared to others.

We acknowledge that, despite the promising biological activities of the *Tilia* species, the lack of data on combination treatments with known anticancer agents such as doxorubicin might be considered a limitation of this study.

Conclusion

In conclusion, this study demonstrated potent and promising anti-inflammatory and anti-cancer activities of different hydroethanolic extracts of chemically characterized *Tilia* species from Türkiye. The anti-inflammatory effects of *Tilia* species rich in phenolic compounds were supported by their strong capacity to reduce nitrite and inhibit IL-6 and PGE_2 release, while selective and dose-dependent cytotoxicity on pancreatic cancer was demonstrated by a significant reduction in viability. Of note, *T. rubra* exerted the highest anticancer effect, with extracts from all parts leading to arrest at the G0/G1 phase. Taken together, this study highlights a potential use for *Tilia* extracts, particularly *T. rubra* with the major quercitrin content, in the prevention and treatment of pancreatic cancer.

Data availability

Corresponding author, Prof. Dr. Hande Sipahi will share the research data supporting the results of our article via the URL link upon request.

Received: 7 June 2024; Accepted: 10 January 2025
Published online: 17 January 2025

References

1. Reuter, S., Gupta, S. C., Chaturvedi, M. M. & Aggarwal, B. B. Oxidative stress, inflammation, and cancer: how are they linked? *Free Radic Biol. Med.* **49**(11), 1603–1616. https://doi.org/10.1016/j.freeradbiomed.2010.09.006 (2010).
2. Rudrapal, M. et al. Dietary polyphenols and their role in oxidative stress-ınduced human diseases: ınsights ınto protective effects, antioxidant potentials and mechanism(s) of action. *Front. Pharmacol.* **13**, 806470. https://doi.org/10.3389/fphar.2022.806470 (2022).
3. Zhang, Y. J. et al. Antioxidant phytochemicals for the prevention and treatment of chronic diseases. *Molecules* **20**(12), 21138–21156. https://doi.org/10.3390/Molecules201219753 (2015).
4. Tanker, N., Koyuncu, M. & Coşkun, M. Pharmaceutical Botany (Course Books, No. 93) (Ankara University Press, Faculty of Pharmacy, 2014).
5. Yeşilada, E. et al. Traditional medicine in Turkey IX: folk medicine in north-west Anatolia. *J. Ethnopharmacol.* **64**(3), 195–210. https://doi.org/10.1016/s0378-8741(98)00133-0 (1999).
6. Riaz, A. et al. Astragalin: a bioactive phytochemical with potential therapeutic activities. *Adv. Pharmacol. Sci.* **2018**, 9794625. https://doi.org/10.1155/2018/9794625 (2018).
7. Grochowski, D. M., Locatelli, M., Granica, S., Cacciagrano, F. & Tomczyk, M. A review on the dietary flavonoid tiliroside. *Compr. Rev. Food Sci. Food Saf.* **17**(5), 1395–1421. https://doi.org/10.1111/1541-4337.12389 (2018).
8. Fitsiou, I., Tzakou, O., Hancianu, M. & Poiata, A. Volatile constituents and antimicrobial activity of *Tilia tomentosa* Moench and *Tilia cordata* Miller Oils. *J. Essent. Oil Res.* **19**, 183–185. https://doi.org/10.1080/10412905.2007.9699255 (2007).
9. Georgiev, Y. N. et al. Acidic polysaccharide complexes from purslane, silver linden and lavender stimulate Peyer's patch immune cells through innate and adaptive mechanisms. *Int. J. Biol. Macromol.* **105**(Pt1), 730–740. https://doi.org/10.1016/j.ijbiomac.2017.07.095 (2017).
10. Formica, J. V. & Regelson, W. Review of the biology of Quercetin and related bioflavonoids. *Food Chem. Toxicol.* **33**(12), 1061–1080. https://doi.org/10.1016/0278-6915(95)00077-1 (1995).
11. Wang, Q. et al. Hyperoside: a review on its sources, biological activities, and molecular mechanisms. *Phytother Res.* **36**(7), 2779–2802. https://doi.org/10.1002/ptr.7478 (2022).
12. Hake, A., Symma, N., Esch, S., Hensel, A. & Düfer, M. Alkaloids from lime flower (Tiliae Flos) exert spasmodic activity on murine airway smooth muscle ınvolving acetylcholinesterase. *Planta Med.* **88**(8), 639–649. https://doi.org/10.1055/a-1534-3766 (2022).
13. Jabeur, I. et al. Contribution of the phenolic composition to the antioxidant, anti-inflammatory and antitumor potential of Equisetum giganteum L. and Tilia platyphyllos Scop. *Food Funct.* **8**(3), 975–984. https://doi.org/10.1039/c6fo01778a (2017).
14. Pietrzak, W., Nowak, R., Gawlik-Dziki, U., Lemieszek, M. K. & Rzeski, W. LC-ESI-MS/MS ıdentification of biologically active phenolic compounds in mistletoe berry extracts from different host trees. *Molecules* **22**(4), 624. https://doi.org/10.3390/molecules22040624 (2017).
15. Barreiro Arcos, M. L. et al. *Tilia cordata* Mill. Extracts and scopoletin (isolated compound): differential cell growth effects on lymphocytes. *Phytother Res.* **20**(1), 34–40. https://doi.org/10.1002/ptr.1798 (2006).
16. Jiménez-González, V., Benítez, G., Pastor, J. E., López-Lázaro, M. & Calderón-Montaño, J. M. Evaluation of anticancer activity of 76 plant species collected in Andalusia (Spain) against lung cancer cells. *Plants* **12**(18), 3275. https://doi.org/10.3390/plants12183275 (2023).
17. Sung, H. et al. Global Cancer statistics 2020: GLOBOCAN estimates of ıncidence and mortality worldwide for 36 cancers in 185 countries. *CA Cancer J. Clin.* **71**(3), 209–249. https://doi.org/10.3322/caac.21660 (2021).
18. Singleton, V. L., Rudolf, O. & Lamuela-Raventós, R. M. Analysis of total phenols and other oxidation substrates and antioxidants by means of folin-ciocalteu reagent. Methods in Enzymology. Academic, Vol. 299. 152–178. https://doi.org/10.1016/S0076-6879(99)99017-1 (1999).
19. Farasat, M., Khavari-Nejad, R. A., Nabavi, S. M. & Namjooyan, F. Antioxidant activity, total phenolics and flavonoid contents of some edible green seaweeds from Northern coasts of the Persian Gulf. *Iran. J. Pharm. Res.* **13**(1), 163–170 (2014).
20. Blois, M. S. Antioxidant determinations by the use of a stable free radical. *Nature* **181**, 1199–1200. https://doi.org/10.1038/1811199a0 (1958).
21. Apak, R., Güçlü, K., Ozyürek, M. & Karademir, S. E. Novel total antioxidant capacity index for dietary polyphenols and vitamins C and E, using their cupric ion reducing capability in the presence of neocuproine: CUPRAC method. *J. Agric. Food Chem.* **52**(26), 7970–7981. https://doi.org/10.1021/jf048741x (2004).
22. Berker, K. I., Güçlü, K., Tor, I. & Apak, R. Comparative evaluation of Fe(III) reducing power-based antioxidant capacity assays in the presence of phenanthroline, batho-phenanthroline, tripyridyltriazine (FRAP), and ferricyanide reagents. *Talanta* **72**(3), 1157–1165. https://doi.org/10.1016/j.talanta.2007.01.019 (2007).
23. Sipahi, H. et al. A comprehensive study to evaluate the wound healing potential of okra (Abelmoschus esculentus) fruit. *J. Ethnopharmacol.* **287**, 114843. https://doi.org/10.1016/j.jep.2021.114843 (2022).
24. Kırmızıbekmez, H. et al. Phenolic compounds from the aerial parts of Clematis viticella L. and their in vitro anti-inflammatory activities. *Nat. Prod. Res.* **33**(17), 2541–2544. https://doi.org/10.1080/14786419.2018.1448815 (2019).
25. Erdogan, M. et al. Secondary metabolites from *Scutellaria brevibracteata* subsp. subvelutina and their in vitro anti-inflammatory activities. *South. Afr. J. Bot. vol.* **139**, 12–18. https://doi.org/10.1016/j.sajb.2021.01.028 (2021).
26. Okur, M. E. et al. Anti-inflammatory, analgesic and in vivo-in vitro wound healing potential of the Phlomis Rigida Labill. Extract. *J. Ethnopharmacol.* **266**, 113408. https://doi.org/10.1016/j.jep.2020.113408 (2021).

27. Coskun, G. P. et al. Discovery of novel thiophene/hydrazones: ın vitro and ın silico studies against pancreatic cancer. *Pharmaceutics* **15**(5), 1441. https://doi.org/10.3390/pharmaceutics15051441 (2023).
28. Čeponytė, U., Paškevičiūtė, M. & Petrikaitė, V. Comparison of NSAIDs activity in COX-2 expressing and non-expressing 2D and 3D pancreatic cancer cell cultures. *Cancer Manag Res.* **10**, 1543–1551. https://doi.org/10.2147/CMAR.S163747 (2018).
29. Guzelmeric, E. et al. Insights into the anti-inflammatory, analgesic, and anticancer potentials of the standardized extracts from three Cistus L. Species. *J. Herb. Med.* **41**, 100724. https://doi.org/10.1016/j.hermed.2023.100724 (2023).
30. Benzie Iris, M. & Devaki The ferric reducing/antioxidant power (FRAP) assay for non-enzymatic antioxidant capacity: concepts, procedures, limitations and applications: Recent Trends and Applications. *Measurement of Antioxidant Activity & Capacity* (pp.77–106). (2017). https://doi.org/10.1002/9781119135388.ch5
31. Toker, G., Aslan, M., Yeşilada, E., Memişoğlu, M. & Ito, S. Comparative evaluation of the flavonoid content in officinal Tiliae flos and Turkish lime species for quality assessment. *J. Pharm. Biomed. Anal.* **26**(1), 111–121. https://doi.org/10.1016/s0731-7085(01)00351-x (2001).
32. Ziaja, M. et al. /MS analysis of extracts from linden flowers (Tiliae Flos): differences in the chemical composition between five Tilia species growing in Europe. *Ind. Crops Prod.* **154**, 112691. https://doi.org/10.1016/j.indcrop.2020.112691 (2020).
33. Song, J. et al. New progress in the pharmacology of protocatechuic acid: A compound ingested in daily foods and herbs frequently and heavily. *Pharmacol. Res.* **161**, 105109. https://doi.org/10.1016/j.phrs.2020.105109 (2020).
34. Luhata, L. P. & Luhata, W. G. Tiliroside: biosynthesis, bioactivity and structure activity relationship (SAR)-A review. *J. Phytopharmacology*. **6** (6), 343–348. https://doi.org/10.31254/phyto.2017.6607 (2017).
35. Valentová, K., Vrba, J., Bancířová, M., Ulrichová, J. & Křen, V. Isoquercitrin: pharmacology, toxicology, and metabolism. *Food Chem. Toxicol.* **68**, 267–282. https://doi.org/10.1016/j.fct.2014.03.018 (2014).
36. Chen, J. et al. Structure-antioxidant activity relationship of methoxy, phenolic hydroxyl, and carboxylic acid groups of phenolic acids. *Sci. Rep.* **10** (1), 2611. https://doi.org/10.1038/s41598-020-59451-z (2020).
37. Elisia, I. et al. Comparison of RAW264.7, human whole blood and PBMC assays to screen for immunomodulators. *J. Immunol. Methods*. **452**, 26–31. https://doi.org/10.1016/j.jim.2017.10.004 (2018).
38. Toker, G., Küpeli, E., Memisoğlu, M. & Yesilada, E. Flavonoids with antinociceptive and anti-inflammatory activities from the leaves of Tilia argentea (silver linden). *J. Ethnopharmacol.* **95**(2–3), 393–397. https://doi.org/10.1016/j.jep.2004.08.008 (2004).
39. Fawzy, G., Younes, K., Waked, E. & Mahmoud, H. Anti-inflammatory, Antinociceptive and nephroprotective activities of *Tilia cordata* and isolation of Bioactive compounds. *J. Mater. Environ. Sci.* **9**(6), 1908–1914. https://doi.org/10.26872/jmes.2018.9.6.210 (2018).
40. Diegelmann, R. F. & Chalfant, C. E. Frontiers in Inflammation, Basic Biology and Clinical Aspects of Inflammation1 (Bentham Science, 2016).
41. Brizi, M. R., Marrassini, C., Zettler, G., Ferraro, G. & Anesini, C. Comparative antiproliferative action of two extracts from tilia x viridis on normal and tumoral lymphocytes: relationship with antioxidant activity. *Chinese Medicine*. Vol.3 No.1. (2012). https://doi.org/10.4236/cm.2012.31005
42. Zheng, Z. et al. The natural compound neobractatin ınduces cell cycle arrest by regulating E2F1 and Gadd45α. *Front. Oncol.* **9**, 654. https://doi.org/10.3389/fonc.2019.00654 (2019).
43. Bailon-Moscoso, N., Cevallos-Solorzano, G., Romero-Benavides, J. C. & Orellana, M. I. Natural compounds as modulators of cell cycle arrest: application for anticancer chemotherapies. *Curr. Genomics*. **18**(2), 106–131. https://doi.org/10.2174/1389202917666160808125645 (2017).
44. Manuele, M. G., Ferraro, G. & Anesini, C. Effect of Tilia x Viridis flower extract on the proliferation of a lymphoma cell line and on normal murine lymphocytes: contribution of monoterpenes, especially limonene. *Phytother Res.* **22**(11), 1520–1526. https://doi.org/10.1002/ptr.2524 (2008).
45. Kavousi, M. & Delfani, A. Solanum pseudo-capsicum effects on bax and bcl-2 gene expression and apoptosis in MCF-7 cell line. *Genetika Vol*. **55 No2**, 523–536. https://doi.org/10.2298/GENSR2302523K (2023).
46. Ferreira, T. et al. Toxicological and anti-tumor effects of a linden extract (Tilia platyphyllos Scop.) In a HPV16-transgenic mouse model. *Food Funct.* **12**(9), 4005–4014. https://doi.org/10.1039/d1fo00225b (2021).

Acknowledgements
The authors would like to thank Ayça Ece Nezir for English language editing.

Author contributions
GY contributed to the conceptualization, data curation, formal analysis, validation, investigation, methodology, and writing of the manuscript. YO, DG, NBŞ, İB and OS contributed to the data curation, formal analysis, validation, investigation, and methodology of the manuscript. GE contributed to investigation. DT and VP contributed to the critical review and editing of the manuscript. EG and HS contributed to the conceptualization, supervision, funding acquisition, data curation, formal analysis, and critical review and editing of the manuscript.

Declarations

Competing interests
The authors declare no competing interests.

Additional information
Supplementary Information The online version contains supplementary material available at https://doi.org/10.1038/s41598-025-86457-2.

Correspondence and requests for materials should be addressed to H.S.